Nano Energy 111 (2023) 108412

Contents lists available at ScienceDirect

Nano Energy

journal homepage: www.elsevier.com/locate/nanoen

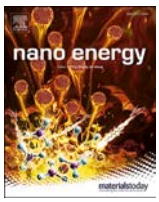

3D spirally coiled piezoelectric nanogenerator for large impact energy harvesting

Binbin Ma [a,b], Li Cheng [a], Suo Bai [a], Xiaofeng Jia [a], Jun Ma [a], Jiling Zhao [a], Longfei Wang [b,*], Yong Qin [a,*]

[a] Institute of Nanoscience and Nanotechnology, School of Materials and Energy, Lanzhou University, Lanzhou 730000, China
[b] Beijing Institute of Nanoenergy and Nanosystems, Chinese Academy of Sciences, Beijing 101400, China

ARTICLE INFO

Keywords:
Piezoelectric nanogenerator
Nanogenerator
Mechanical energy harvesting
Large impact pressure
Spirally coiled structure

ABSTRACT

Piezoelectric nanogenerator is an emerging technology that can convert irregular discrete mechanical energy in the environment into electricity, which provides a long-term continuous power supply solution for mobile distributed electronics. However, it is still difficult to effectively harvest the large impact mechanical energy. Here, we developed a new kind of three-dimensional spirally coiled piezoelectric nanogenerator (SC-PENG), which can effectively convert irregular axial impact forces into uniform radial pressures, and achieve large-scale impact mechanical energy harvesting (corresponding pressures range from 80 kPa to 6.32 MPa). Especially, under a large impact pressure of 3.05 MPa, the output current, voltage and the equivalent transfer charge density of SC-PENG is up to 196 μA, 36 V and 2550 μC m^{-2} respectively, which break the record of PENG among previous studies. The volume of the piezoelectric film and the corresponding volume charge density are 0.224 cm^{-3} and 580 nC cm^{-3}, respectively. Moreover, factors such as particle connectivity and modulus of the piezoelectric film are explored in detail, which can further improve the electromechanical conversion capability of PENG. This work not only achieves high electrical output of PENG, but also paves an efficient strategy for large impact mechanical energy harvesting towards practical application.

1. Introduction

With the rapid development of human information society, large numbers of distributed mobile electronics are widely used in industrial production and daily life [1,2]. Developing a new power supply way that can keep electronics working stably for a long time is extremely urgent. As a new electromechanical conversion technology based on piezoelectric effect, piezoelectric nanogenerator (PENG) that can convert the discrete and low-frequency irregular mechanical energy in the surrounding environments into electricity draws lots of attention, and has made important progress in the fields of mechanical energy harvesting and self-powered sensing system [3–7]. PENG has the advantage of stable output without interference from environmental temperature, humidity, and other factors [8–10], providing a reliable option for the continuous power supply of the Internet of Things electronics. However, due to the limited piezoelectric and mechanical properties of piezoelectric nanowires or composite films, only a specific range of weak mechanical energy can be harvested, and the output current of PENG remains low, which severely hinders their practical applications, especially in large impact energy harvesting in our life.

To enhance the output of PENG, a series of schemes and technologies have been proposed, such as integration of nanowire arrays [11–13], multi-device series-parallel connection [14,15], selecting or synthesizing materials with strong piezoelectricity [8,16–18], dielectrophoresis and frozen template casting [19–21] and so on. Based on the above methods, the output voltage and current of PENGs have been increased from 8 mV to 250 V, and from 0.4 nA to 353 μA, respectively [3,8,22–24], and the equivalent surface charge density reaches 1690 μC m^{-2}. It can be concluded from these efforts that the core of improving output is to improve the effective piezoelectricity of piezoelectric modules. Compared with materials such as piezoelectric nanowires and ultrathin piezoelectric ceramic sheets with complicated preparation processes, piezoelectric composite films have been investigated emphatically because of their outstanding flexibility, wide material choice, and simple preparation process *etc* [25–29], and the content of piezoelectric particles in the composite films is easy to adjust, which can improve the

* Corresponding authors.
E-mail addresses: lfwang12@binn.cas.cn (L. Wang), qinyong@lzu.edu.cn (Y. Qin).

https://doi.org/10.1016/j.nanoen.2023.108412
Received 15 February 2023; Received in revised form 23 March 2023; Accepted 31 March 2023
Available online 1 April 2023

output of PENG and have a wider application. Piezoelectric composite films consist of piezoelectric particles with excellent piezoelectric properties and highly flexible polymers, in which the connectivity of piezoelectric particles and the mechanical properties of polymer matrix are the keys to improve the output of composite films. The introduction of dielectrophoresis or frozen template casting in the preparation of films can substantially enhance the connectivity of particles, and the mechanical properties of films can also be improved by selecting high modulus polymer matrix with proper thickness [30,31]. Nevertheless, a certain number of piezoelectric particles agglomeration and many non-uniform inorganic particle-polymer interfaces still exist due to the density and surface states difference between piezoelectric particles and polymer molecules. This situation leads to the stress concentration of the composite film, which results in the film not being able to bear excessive external force [32].

On the other hand, the development of PENGs with novel structures can also improve the output, such as curved-type [33], three-dimensional (3D) interdigital electrode structure [24,34], and rugby ball-structured [23]. Effective prestress and proper geometric structure provide a basis for more efficient energy harvesting. In particular, 3D structures have special mechanical properties of spatial structures, for example, the cymbal-type structure [35,36] can

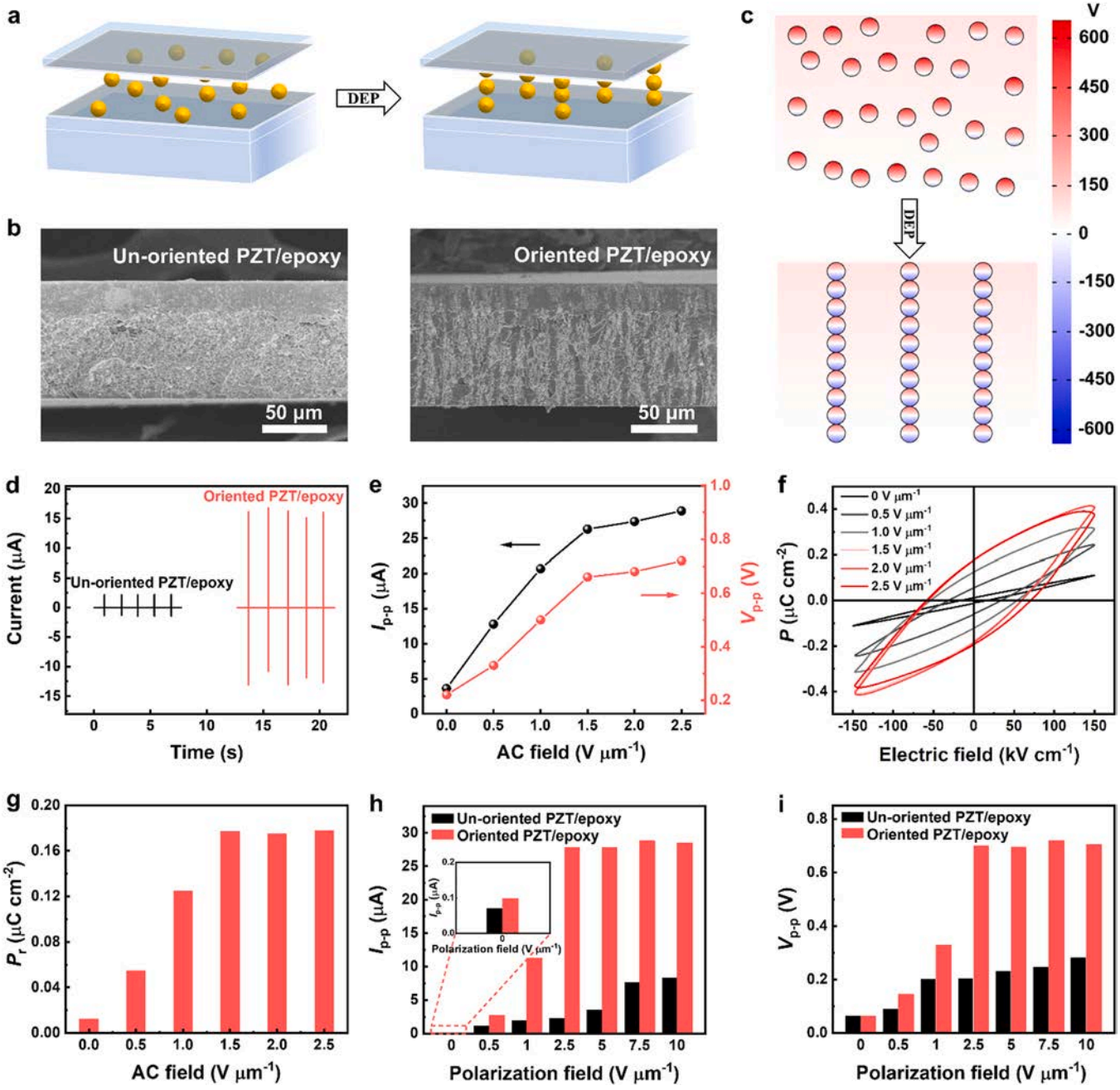

Fig. 1. Characterization of the PZT/epoxy resin composite film and the effect of dielectrophoresis (DEP) AC fields on the film properties. a Schematic diagram of the preparation of oriented PZT/epoxy film using DEP. b SEM images of the cross-section of the un-oriented and oriented PZT/epoxy films. c Potential distribution of un-oriented and oriented composite films in a polarized electric field. d The output current of un-oriented and oriented films. e Variation trends of output current and voltage (peak to peak value) of PZT/epoxy films under different AC fields. f and g Polarization–electric field (P-E) hysteresis loops and remnant polarization (P_r) of PZT/epoxy films treated by DEP in different AC fields. h and i Peak-to-peak value variation of output current and voltage for un-oriented and oriented PZT/epoxy films with increasing polarization field.

withstand dynamic heavy loads by turning the axial force into the radial force, which means that it can collect a wide range of mechanical energy, especially in large impact mechanical energy. Therefore, effective harvesting of large impact mechanical energy can be achieved from two aspects: optimizing composite film piezoelectricity and constructing 3D structure.

In this work, we developed a three-dimensional spirally coiled piezoelectric nanogenerator (SC-PENG), which can harvest a wide range of impact mechanical energy more effectively (corresponding pressures range from 80 kPa to 6.32 MPa). Specifically, under a large impact pressure of 3.05 MPa, the output current and voltage of SC-PENG are 196 μA and 36 V, respectively. The equivalent transfer charge density reaches 2550 μC m^{-2}, which is 1.5 times the record of PENG in literatures. In addition, dielectrophoresis technology and epoxy resin with high modulus are introduced to prepare a highly flexible PZT/epoxy piezoelectric composite film with excellent piezoelectricity, which can further improve the output performance of PENG. Our study provides a promising strategy for achieving high performance PENGs for large-scale impact mechanical energy collection in practical applications.

2. Results and discussion

2.1. Optimization of the connectivity of PZT particles in PZT/epoxy film

Reducing the agglomeration and improving the connectivity of piezoelectric particles in polymers is an effective way to ensure the piezoelectricity of ceramic-polymer composite films. Here, we use dielectrophoresis (DEP) to improve the connectivity of PZT particles in the PZT/epoxy film (the process schematic of DEP shown in Fig. 1a). The irregularly shaped PZT particles are subject to an inhomogeneous Coulomb force from periodic vibrations during the curing process of the epoxy, which promotes the PZT particles to turn and move slightly and finally form a linear distribution. Fig. 1b shows the cross-sectional SEM images of the PZT/epoxy film before and after DEP, of which the PZT changes from an unordered random distribution state to an oriented connected structure with linear distribution. The finite element analysis is used to simulate the polarization potential distribution of the PZT/epoxy film before and after DEP, as shown in Fig. 1c. The potential difference between the two ends of oriented PZT particles increases substantially, which promotes the effective polarization of PZT particles. Then, we characterized the output of un-oriented and oriented PZT/epoxy film based nanogenerators (Fig. 1d). The output current peak of the oriented PZT/epoxy film is about 16.4 μA, which is about 8 times that of the un-oriented film. Figs. 1e and S3 show the variation trend of the peak-to-peak values of current and voltage ($I_{p\text{-}p}$ and $V_{P\text{-}P}$) versus the strength of electric field, indicating that the AC field strength employed by the DEP can directly affect the orientation of PZT particles. The output of the PZT/epoxy film shows a linear increase in the intensity of the AC field less than 1.5 V μm^{-1}. With the AC field increasing to 2.5 V μm^{-1}, the increasing trend of PZT/epoxy film output began to become slow. Furthermore, we explored the changes of the polarization-electric field (P-E) hysteresis loop (Fig. 1f) of PZT/ epoxy films prepared by different AC field treatments. Comparing the corresponding remnant polarization (P_r) of different PZT/epoxy films (Fig. 1g), the variation trend is consistent with that of the output current, the remnant polarization of the well-oriented PZT/epoxy film is 0.177 μC cm^{-2}, which is 14 times higher than the un-oriented PZT/epoxy film, indicating that the improvement of PZT particle connectivity increases the piezoelectricity of the PZT/epxoy film. Besides, the piezoelectric coefficient of un-oriented PZT/epoxy film is 0.3 pC N^{-1} and increased to 2.9 pC N^{-1} after orientation treatment, which also shows the enhancement of piezoelectricity of PZT/epoxy film. In order to investigate the effect of polarization field intensity on output of unoriented and orientated PZT/epoxy film, different intensity of 0, 0.5, 1.0, 2.5, 5.0, 7.5, and 10.0 V μm^{-1} are applied, and the results are shown in Figs. 1h,i and S4. It can be observed that polarization of the oriented PZT/epoxy film has been completed under the polarization field of 2.5 V μm^{-1}, and the output tends to be stable as the increase of intensity. Nevertheless, the output of un-oriented PZT/epoxy film increases synchronously with increase of polarization field intensity, which is only 1/3 that of the oriented PZT/epoxy film under a polarization field of 10.0 V μm^{-1}. A PZT/epoxy film with well-oriented PZT particles forms a continuous linear structure, and the significant improvement in PZT connectivity benefits the polarization of PZT particles and improves the transport path of the force. Thus, the well-oriented PZT can generate larger deformations compared to un-oriented PZT/epoxy films, which is advantageous to increase the output performance of PENG.

2.2. Improvement of the PZT/epoxy film's mechanical properties

The Young's modulus of the piezoelectric composite film directly affects the transfer of the applied force. A high modulus of the composite film could help to improve the output of PENG [37]. Compared with mainstream composite film matrix polymers such as polydimethylsiloxane (PDMS) and poly(vinylidene difluoride) (PVDF), epoxy resin has the advantages of controllable modulus, high strength and excellent chemical resistance [38,39]. Hence, the mechanical energy harvesting efficiency of PENG can be improved by optimizing and improving the Young's modulus of epoxy matrix. At first, seven kinds of epoxy films were prepared by adjusting the ratio of prepolymer SL3010A, prepolymer SL3423 and curing agent SL3010B respectively. With the increase of the relative content of prepolymer SL3010A, those epoxy resin films were named as epoxy 1 to epoxy 7 respectively (see Table S1 for details). The stress-strain curves of seven kinds of epoxy films are shown in the Fig. S5. The elastic strain range decreases and the curve slope of the corresponding films increases substantially with the increase of the relative content of the high-density prepolymer SL3010A, which indicates that the Young's modulus of the epoxy film increases. The corresponding Young's modulus of the epoxy film is calculated to be 1.4, 56, 122, 330, 414, 556, and 2420 MPa, and the results are shown in the black histogram in Fig. 2b. Subsequently, the stress-strain curves of seven kinds of PZT/ epoxy composite films after adding PZT particles were also explored, and the results are shown in Fig. 2a, where the slope of the PZT/epoxy film curves slowly increases with increasing modulus of the epoxy matrix. The modulus of PZT/epoxy film increases synchronously compared with that of pure epoxy film, and the corresponding Young's modulus of PZT/ epoxy film increases to 1.9, 64, 144, 380, 695, 912 and 3260 MPa respectively. Furthermore, we characterized the output of PENG based on different Young's moduli PZT/epoxy film, and the output current and output voltage change trend as shown in the Figs. 2c,d and S6, which indicates that the increase of PZT/epoxy film modulus effectively improves the output of PENG. To sum up, the Young's modulus and fracture toughness of the PZT/epoxy film are improved by using high-density prepolymer SL3010A and adding PZT particles with linear distribution both strengthen particle bridging effect and interlocking effect [40,41], which can enhance the transmission effect of external forces and hence improve the output of PENG.

2.3. Output performance of the typical sandwich structure PENG

To characterize the output performance of the optimized PZT/Epoxy film, we fabricate the PENGs with typical sandwich structure as shown in the schematic diagram (Fig. 3a), which illustrates the distribution state of PZT particles in the composite film. The experimental results of output current and voltage of the PENGs under different pressures are shown in Fig. 3b,c. As the pressure increases from 0.32 MPa to 1.66 MPa, the output current and voltage increase from 8.8 μA and 5.4 V to 212 μA and 74 V, respectively. The maximum current density of the PZT/epoxy film reaches 126 μA cm^{-2}, which is much higher than the record among the ceramic-polymer composite film based PENGs in literature (Fig. S7). However, to further increase the applied stress, the PENG cannot continue to work properly since the PZT/epoxy film start

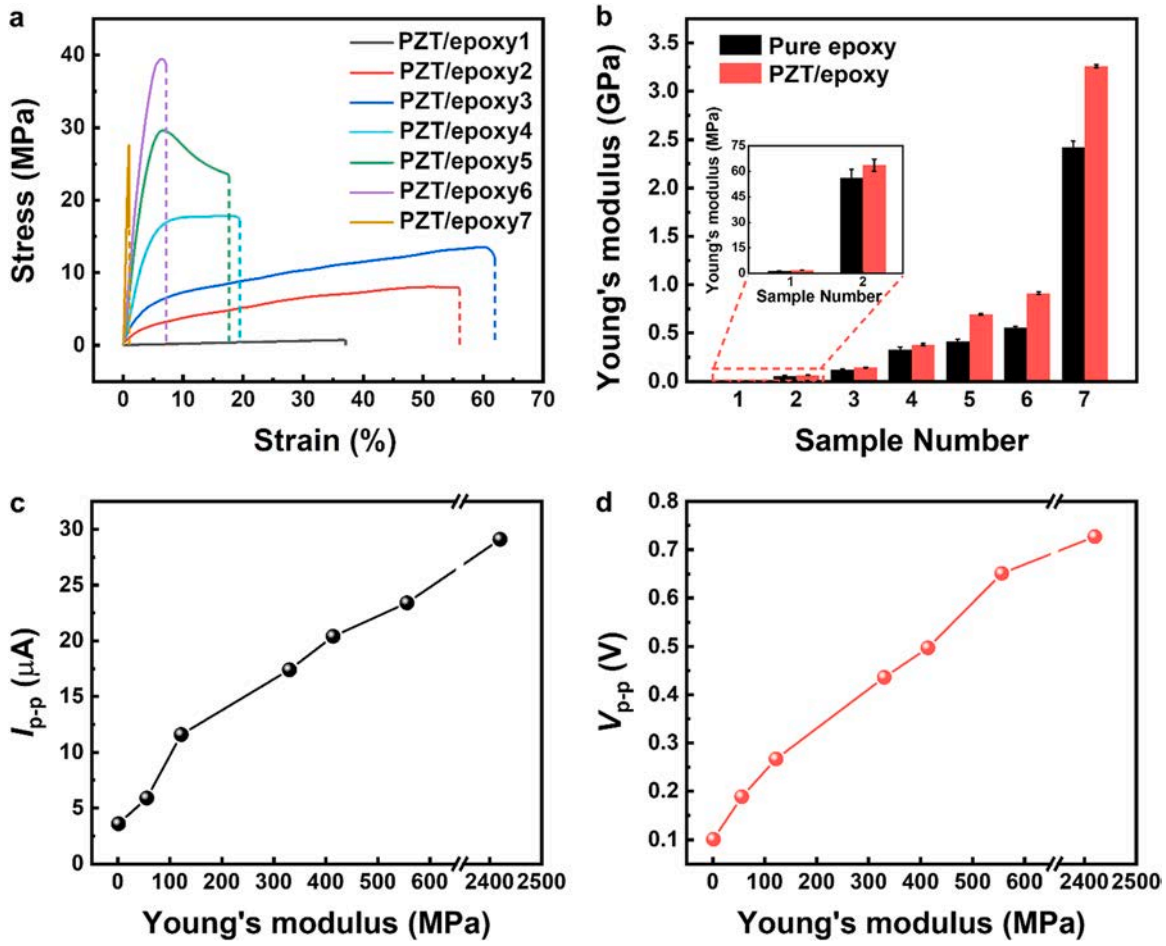

Fig. 2. Mechanical properties of PZT/epoxy films and effect on the electric output performance. a and b Stress-strain curves and corresponding Young's modulus of different epoxies. c and d Variation trend of output performance of PZT/epoxy films with increasing epoxy modulus of PZT/epoxy composite films.

to damage. Fig. 3d(i) shows the stress distribution within PZT/epoxy films under small and large impact pressure respectively. Regardless of the impact pressure size, the stress area of the device is mainly concentrated in the contact area with the external force, and the maximum pressure appears at the contact boundary, which makes the boundary prone to stress concentration. Even though the stress concentrations will appear at the contact boundary under small pressure, it is not enough to damage the device, and hence can harvest mechanical energy normally. With the rapid increase of external pressure, the stress concentrations of device at the contact boundary increase significantly, and the PZT/epoxy film itself stress concentration further aggravates the stress concentration of the contact boundary, which leads to the device fracture and results in PENG incapability of working under large impact pressure.

2.4. Design of SC-PENG to harvest large impact mechanical energy

In order to harvest large impact mechanical energy more effectively, it is the key to reduce the stress concentration of devices. Here, a 3D spirally coiled structure is constructed to change the pressure distribution of the PZT/epoxy film as shown in Fig. 3d(ii). When the convex spherical part at the top of the super-elastic rubber column is subjected to external impact pressure, it can turn the impact pressure into radial outward pressure to drive the PZT/epoxy film wound around the super-elastic rubber column to deform, which avoids the direct contact between the external impact pressure and the PZT/epoxy film and homogenizes the pressure of the PZT/epoxy film. Compared with the pressure distribution of the PZT/epoxy film of 3D structure and flat structure, the stress concentration of the PZT/epoxy film is obviously reduced. The 3D structure enhances the ability to resist impact pressure, and it can more effectively harvest large impact mechanical energy. To demonstrate the practical performance of 3D structure design, a new kind of 3D spirally coiled piezoelectric nanogenerator (SC-PENG) is developed (Figs. 3e and S8), which consists of a PDMS column with a bulbous structure at the top, a double-layer PZT/epoxy film wound on the PDMS column, and polycarbonate outside the PZT/epoxy film to provide rigid restraint. The double-layer PZT/epoxy film is coiled to construct alternating positive and negative polarization directions, which improves the utilization rate of radial pressure and can harvest mechanical energy more effectively. When the bulbous end of PDMS is pressed, the radial pressure of the middle annular surface is maximum, and presents a decreasing distribution from the center to the edge of PDMS column. Subsequently, the output performance of 3D SC-PENG with optimized electrode (Fig. S9) and typical sandwich structure PENG under different impact pressures are characterized (Figs. 3f and S10). The planar PENG can only harvest mechanical energy within a relative small pressure range (less than 2 MPa) and more sensitive under weak external force, whereas the SC-PENG can harvest energy under a wide range of impact pressure and more efficient in large impact pressures (larger than 6 MPa). The transfer charge density of SC-PENG can even reach 29. 6 nC cm^{-2} under an impact pressure of 6.32 MPa. The results indicate that SC-PENG is more suitable for harvesting large impact mechanical energy owing to the unique 3D structure.

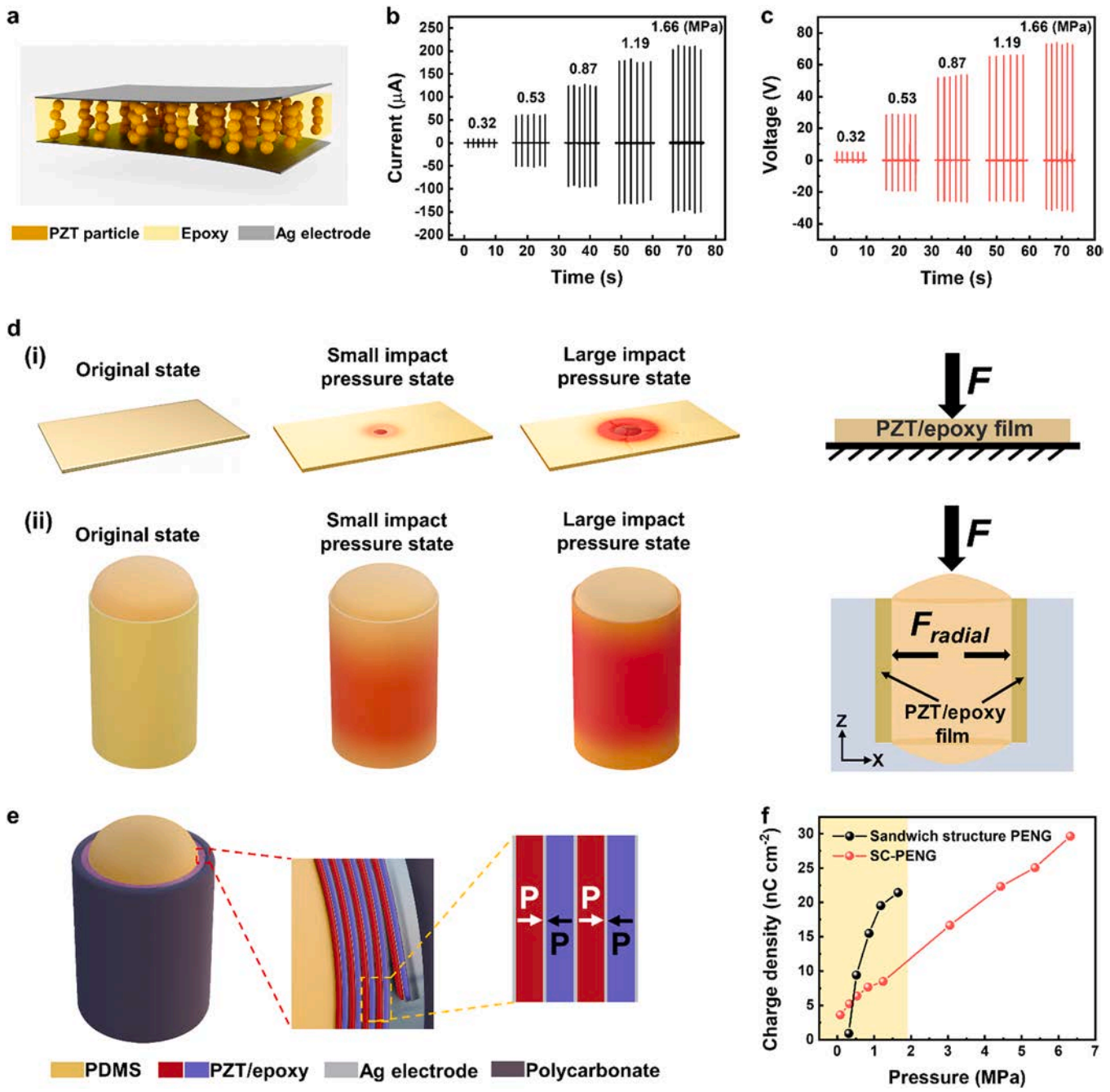

Fig. 3. Output performance of the sandwich structure PENG and advantages of SC-PENG. a Schematic diagram of the sandwich structure PENG. b and c The output current and voltage of the sandwich structure PENG at various impact pressure. d Stress distribution diagram and structural analysis of the flat structure and coiled structure of PZT/epoxy film under small and large impact pressures. e Structure diagram of SC-PENG. f The transfer charge density of the sandwich structure PENG and SC-PENG under different impact pressures.

2.5. *Output performance and application of SC-PENG*

To further improve the output performance of SC-PENG, the effect of coil number of a double-layer PZT film on the output was explored (Fig. 4a,b). With the number of coils increases from 1 to 5, the output current gradually increases from 19.5 μA to ~98 μA, whereas the output voltage decreases from 39 V to 18.4 V. Although the peak current reaches the maximum of 98 μA at 4 coils, the peak-to-peak value of current is close to that of SC-PENG with 5 coils, which are 176.8 μA and 176 μA, respectively. More coils provide more working area, which means that more surface polarized charges can be generated, resulting in higher output current and transfer charge density, which is also shown in Fig. 4c. As the number of coils increases, the radial pressure decreases along the thickness direction and the polarized charge generated by the outer layer PZT/epoxy films gradually decreases compared with the single-coiled state. Since the electrodes are shared, the overall output voltage will be reduced after the system is balanced [24]. Further increasing the number of coils will aggravate the attenuation of output voltage, which impedes the practical application of the SC-PENG. Thus, we choice 5 coil in the following research. Fig. 4d,e show the output current and voltage of the SC-PENG with 5-coil under an impact pressure of 3.05 MPa, namely 196 μA and 36 V. The corresponding transfer charge density is about 2550 μC m^{-2}, which is much higher than the previously reported PENGs in literatures [24,42–46] (Fig. 4f). In order to

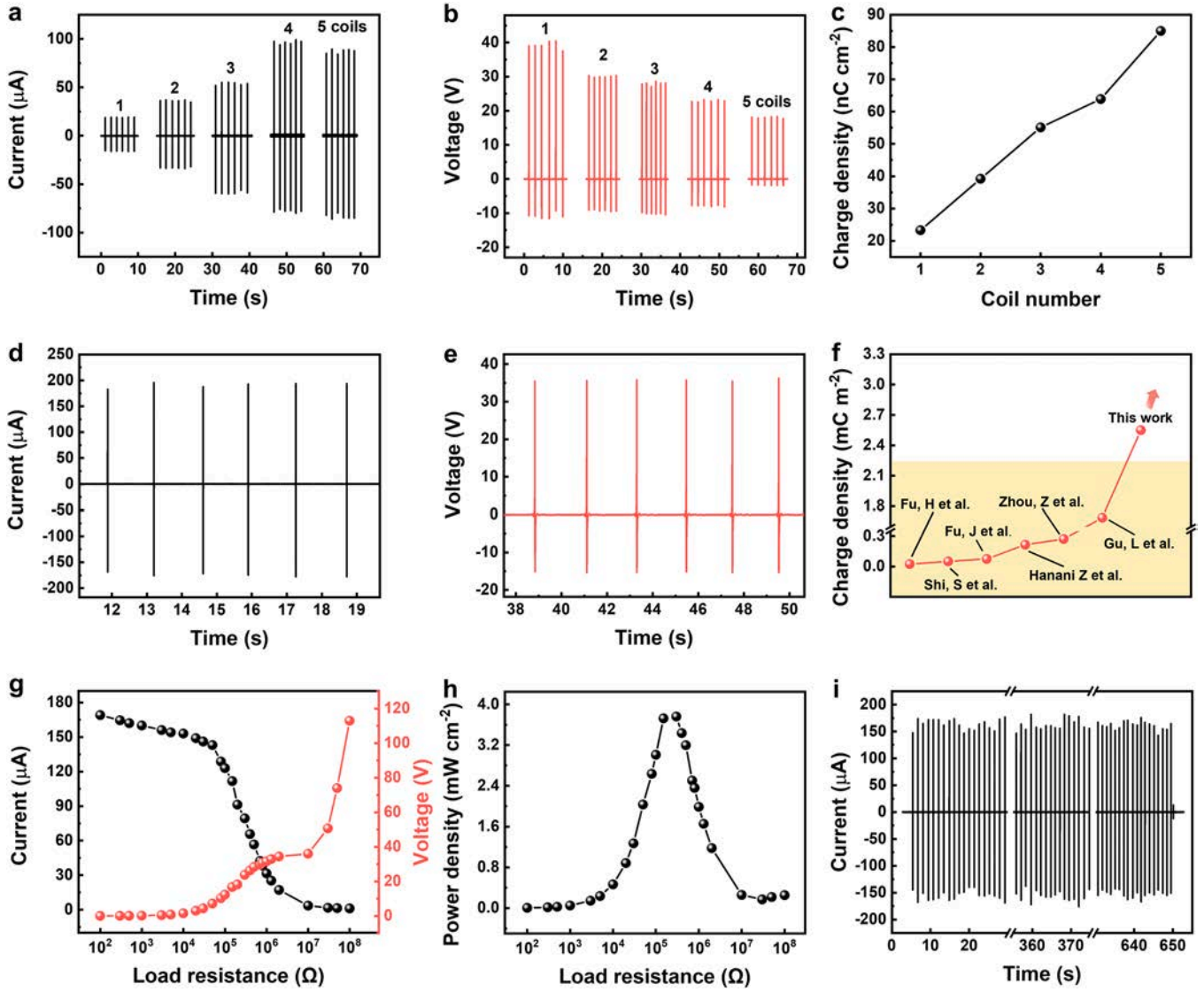

Fig. 4. Output performance of the SC-PENG. a and b The output current and voltage of the SC-PENG fabricated by one to five coiling under dynamic impact pressure of 0.53 MPa. c The trend of the transfer charge density calculated from current signals as increasing number of coils. d and e The current and voltage of SC-PENG with five coils PZT/epoxy film at impact pressure of 3.05 MPa. f Comparison of the transfer charge density of SC-PENG (calculated from the current curve in d) with some representative PENGs. g The trend of the current and voltage of the SC-PENG on the external load resistance under a dynamic pressure of 3.05 MPa. h The peak power density at the external load resistance. i The output stability of SC-PENG under multiple cycles at the impact pressure of 3.05 MPa.

find out the equivalent internal resistance of the SC-PENG and the corresponding maximum output power density, the load peak currents and voltages (Fig. 4g) are measured under a series of external loads. According to the power formula: $P = I^2R$, the output peak power density of the SC-PENG reaches ~3.72 mW cm^{-2} with an external load of 0.15 MΩ (Fig. 4h), which is close to the theoretical maximum power density (~3.75 mW cm^{-2}) at a theoretical optimal load resistance (~0.23 MΩ) (Fig. S11). In addition, The output performance of SC-PENG at different impact frequencies is also explored, showing excellent mechanical energy harvesting ability at different frequencies (Fig. S12). The stability and reliability of SC-PENG are also examined. After enduring multiple cyclic impact pressures, no obvious degradation of the output current is observed (Figs. 4i, S13), which indicates the stability of SC-PENG. Above results demonstrate that the SC-PENG can harvest large impact mechanical energy more effectively.

Large impact mechanical energy can be seen everywhere in life, for example, the mechanical vehicles or people moving can generate a wide range of impact pressure from a few newtons to hundreds of thousands of newtons. If a SC-PENGs array is constructed as envisaged in Fig. 5a, a self-powered system for electrical equipment could be achieved. To demonstrate the potential applications of SC-PENGs for harvesting large impact mechanical energy, we first compare the output of the typical multilayer stacked integrated PENG and SC-PENG with equivalent working area under a pressure of a 70 kg adult fast running (Fig. 5b). The multilayer stacked PENG is gradually damaged under continuous trampling, whereas the SC-PENG can stably and continuously harvest the mechanical energy generated by fast running, showing the advantages of SC-PENG in harvesting large impact mechanical energy. Afterwards, an array of SC-PENGs is constructed, and the output of SC-PENG array at different human motion speeds is characterized (Fig. 5c,d). The peak current and voltage can reach up to ~15 μA and ~40 V under normal walking, which enable lights 27 green LEDs without any circuit management (Fig. 5e), and output can be further increased to ~32 μA and ~80 V under fast running. Furthermore, with the use of full-wave rectifier, the electric energy captured by fast running is stored in 1 μF and 47 μF capacitor (Fig. 5f,g and h), respectively. The charge generated by each step at fast running is calculated to be 130 nC with a corresponding charge density as 517 μC m^{-2}. The variation of the voltage of

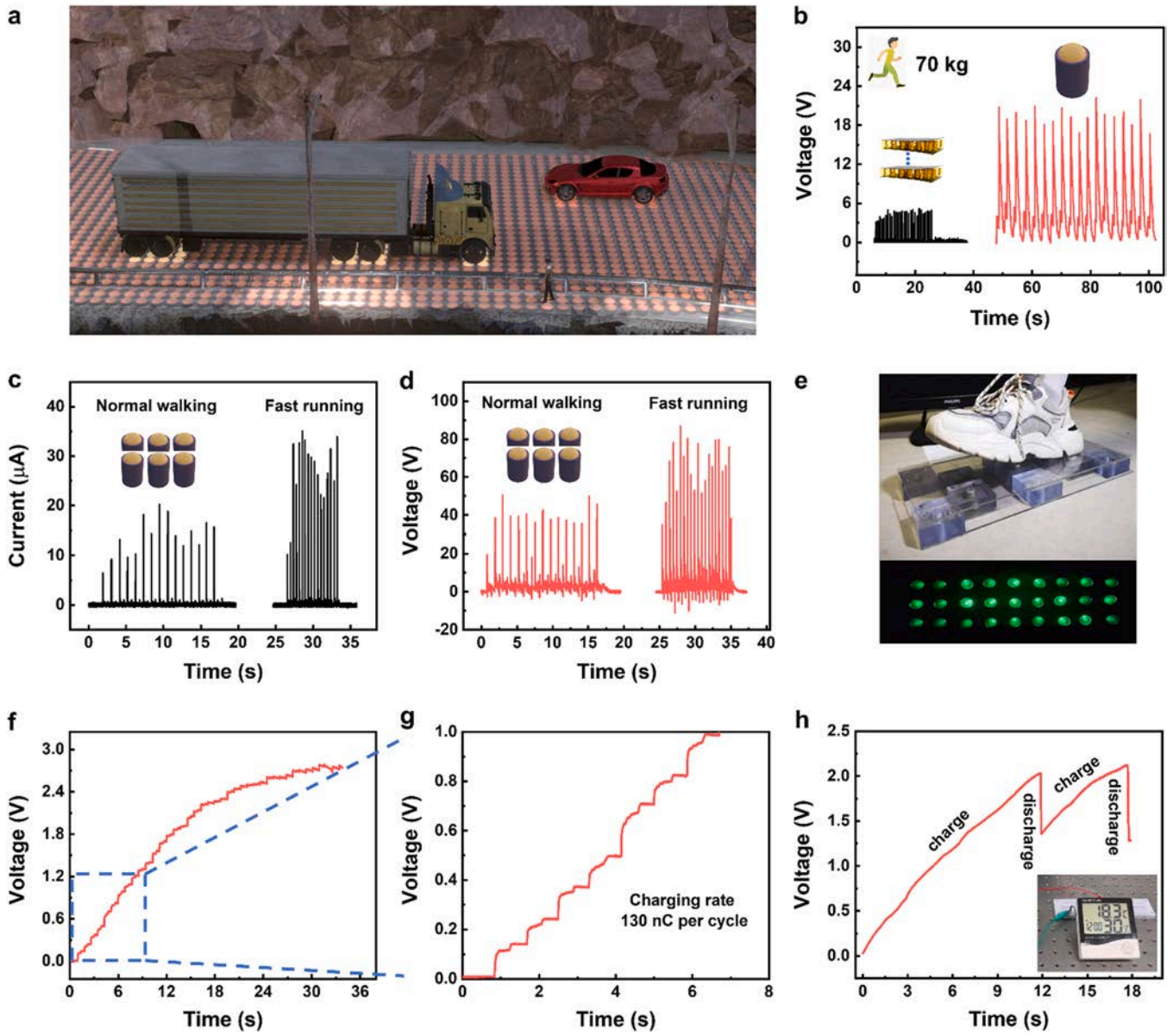

Fig. 5. Application demonstration of the SC-PENG for harvesting large impact mechanical energy. a Schematic diagram of large impact energy harvesting on roads. b Output of the multilayer stacked integrated PENG and SC-PENG during a 70 kg adult fast running. c and d Output of SC-PENG array during normal walking and fast running. e SC-PENG array can directly light 27 green LEDs without rectification under normal walking. f The charging curve for a 1 μF capacitor after rectified under fast running. g The corresponding charging rate calculated as 130 nC per cycle. h The charging and discharging curve for a 47 μF capacitor, inset: the photography for powering a temperature hygrometer.

47 μF capacitor during the charging and discharging process (Fig. 5h), and discharge process of capacitor corresponds to power supply for a commercial temperature hygrometer (inset in Fig. 5h). The applications above can strongly prove the high-output performance of SC-PENGs for large impact mechanical energy harvesting. It could further generate large output energy by optimizing the structural design, increasing the array density of SC-PENG.

3. Conclusions

To summarize, we developed a new kind PENG with spirally coiled structure, which can convert irregular axial impact forces into uniform radial pressures and hence effectively harvest large-scale impact mechanical energy (corresponding pressures range from 80 kPa to 6.32 MPa). Specifically, under a large impact pressure of 3.05 MPa, the output current and voltage of SC-PENG are 196 μA and 36 V, respectively. The equivalent transfer charge density reaches 2550 μC m^{-2}, which is 1.5 times the record of PENG in literatures. Additionally, the output of PENG is further improved by using dielectrophoresis to improve the connectivity of PZT particles in the film and selecting high-modulus epoxy resin to enhance the force transmission ability of the film. This work provides a promising strategy for achieving high performance PENGs for large-scale impact mechanical energy harvesting in practical applications.

4. Experimental section

4.1. Preparation of PZT/epoxy composite films

Lead zirconate titanate powder particles with an average diameter of 1 μm were purchased from Baoding Hongsheng Acoustic Electronic Equipment Co., Ltd. (China) (Characterized in Fig. S1). The epoxy

selected for the present investigation is based on two optically transparent component systems (SL3010, Zhuzhou Shilin Polymer Co., Ltd. China). SL-3010A and SL-3010B are prepolymer and curing agent, the soft resin SL-3423 is used as toughening agent to adjust the Young's modulus of epoxy film. First, SL-3010A and SL-3423 prepolymers were mixed with various weight ratios and then the appropriate amount of PZT powder was added to stirring. Next, the curing agent SL-3010B was added to the mixed slurry and stirred continuously. After the PZT particles, prepolymer and curing agent were sufficiently and uniformly mixed, the slurry was put into the vacuum equipment to remove the bubbles generated by stirring. Finally, the slurry was poured on ITO glass with a certain groove, and another ITO glass was lightly overlapped on the top surface of the slurry. AC fields of different intensities were introduced into the two ITO glasses for dielectrophoresis at a frequency of 50 Hz. Finally, the mixed slurry is wholly cured, and the PZT/epoxy composite film was obtained by peeling it out of the two ITO glasses.

4.2. Fabrication of the flat PENGs and the SC-PENGs

The PZT/epoxy film was cut into a dimension of 2.5 × 1.6 cm^2 and then conductive silver paint was sprayed (Shenzhen Jingzhe technology co., ltd. China) to form coating (2.1 × 0.8 cm^2) as the bottom and top electrodes. Narrow strips of Al foil were attached on the electrodes as wire by ultra-thin conductive adhesive with a thickness less than 10 μm, and the sandwich structure PENG was fabricated. As for the SC-PENG, two PZT/epoxy films were coiled into a coiled structure using a metal rod with a diameter of 8 mm as the core, and then the metal rod was removed from the double piezoelectric layer device with a tubular hollow structure. Then the double piezoelectric layer device was put into a polycarbonate plate with a circular groove, and a PDMS column prepared by template method with bulbous structure was inserted into the hollow area of the double piezoelectric layer device. Then an appropriate amount of PDMS was added for bonding, and epoxy was added into the gap between the double piezoelectric layer device and the polycarbonate plate. The SC-PENG was obtained after the epoxy and PDMS were completely cured, and the detailed device preparation process is shown in Fig. S14. Finally, the sandwich structure PENG and SC-PENG were electrically polarized at 90 °C under 5 kV mm^{-1} for 60 min.

4.3. Characterization and measurement

The morphology of PZT and PZT/epoxy composite films was obtained by field emission SEM (Hitachi S-4800). Ferroelectric hysteresis loop was observed via a standard ferroelectric testing system (aix ACCT, TF Analyzer 3000) at room temperature. The stress-strain curve was measured by a universal testing machine (Instron 3343 material testing machine). The short-circuit current of PENG was measured by a low-noise current amplifier (Stanford, SR570), and the open-circuit voltage of PENG was measured by a data acquisition card (National Instrument BNC-2120).

CRediT authorship contribution statement

Y.Q. and S.B. conceived the project. L.F.W., B.B.M., L.C., and S.B. designed the experiments. B.B.M., X.F.J., J.M., and J.L.Z. performed the experiments. L.F.W., Y.Q., B.B.M., L.C., and S.B. analyzed the results. All authors contributed to discussions and writing of the manuscript.

Declaration of Competing Interest

The authors declare that they have no known competing financial interests or personal relationships that could have appeared to influence the work reported in this paper.

Data availability

Data will be made available on request.

Acknowledgments

This research was supported by the National Key Research and Development Project from Ministry of Science and Technology (2021YFA1201602), the National Natural Science Foundation of China (Nos. 52102067, U21A20175), the Natural Science Foundation of Gansu (No. 21JR7RA490), the National Program for Support of Top-notch Young Professionals.

Appendix A. Supporting information

Supplementary data associated with this article can be found in the online version at doi:10.1016/j.nanoen.2023.108412.

References

[1] J. Yick, Biswanath Mukherjee, Dipak Ghosal, Wireless sensor network survey, Comput. Netw. 52 (12) (2008) 2292–2330.
[2] J. Gubbi, Rajkumar Buyya, Slaven Marusic, Marimuthu Palaniswami, Internet of things (IoT): a vision, architectural elements, and future directions, Future Gener. Comput. Syst. 29 (7) (2013) 1645–1660.
[3] Z.L. Wang, Jinhui Song, Piezoelectric nanogenerators based on zinc oxide nanowire arrays, Science 312 (5771) (2006) 242–246.
[4] S.Q. Xu, Y. Xu, C. Wei, Y. Yang, R. Wang, Z. L, Self-powered nanowire devices, Nat. Nanotechnol. 5 (5) (2010) 366–373.
[5] F.R.T. Fan, Z.L. W. Wang, Flexible nanogenerators for energy harvesting and self-powered electronics, Adv. Mater. 28 (22) (2016) 4283–4305.
[6] Z. Yang, Shengxi Zhou, Jean Inman Zu, Daniel, High-performance piezoelectric energy harvesters and their applications, Joule 2 (4) (2018) 642–697.
[7] W.L. Liu. Y, Yu.X. Zhao. L, Y.L. Zi, Recent progress on flexible nanogenerators toward self-powered systems, InfoMat 2 (2) (2020) 318–340.
[8] K.I.S. Park, J.H. Hwang, G.T. Jeong, C.K. Ryu, J. Koo, M. Choi, I. Lee, S.H. Byun, M. Wang, Z.L. Lee, K. J, Highly-efficient, flexible piezoelectric PZT thin film nanogenerator on plastic substrates, Adv. Mater. 26 (16) (2014) 2514–2520.
[9] H. Chen, L. Zhou, Z. Fang, S. Wang, T. Yang, L. Zhu, X. Hou, H. Wang, Z.L. Wang, Piezoelectric nanogenerator based on in situ growth all-inorganic $CsPbBr_3$ perovskite nanocrystals in PVDF fibers with long-term stability, Adv. Funct. Mater. 31 (19) (2021) 2011073.
[10] D.W. Jin, Y.J. Ko, C.W. Ahn, S. Hur, T.K. Lee, D.G. Jeong, M. Lee, C.Y. Kang, J. H. Jung, Polarization- and electrode-optimized polyvinylidene fluoride films for harsh environmental piezoelectric nanogenerator applications, Small 17 (14) (2021) 2007289.
[11] Y.W. Qin, X. Wang, Z.L. Microfibre-nanowire, hybrid structure for energy scavenging, Nature 451 (7180) (2008) 809–813.
[12] J. Fang, H. Niu, H. Wang, X. Wang, T. Lin, Enhanced mechanical energy harvesting using needleless electrospun poly(vinylidene fluoride) nanofibre webs, Energy Environ. Sci. 6 (7) (2013) 2196–2202.
[13] A. Koka, H.A. Sodano, High-sensitivity accelerometer composed of ultra-long vertically aligned barium titanate nanowire arrays, Nat. Commun. 4 (1) (2013) 2682.
[14] G. Zhu, A.C. Wang, Y. Liu, Y. Zhou, Z.L. Wang, Functional electrical stimulation by nanogenerator with 58 V output voltage, Nano Lett. 12 (6) (2012) 3086–3090.
[15] S. Lee, J.I. Hong, C. Xu, M. Lee, D. Kim, L. Lin, W. Hwang, Z.L. Wang, Toward robust nanogenerators using aluminum substrate, Adv. Mater. 24 (32) (2012) 4398–4402.
[16] C.K. Jeong, Kim Insu, Park Kwi-Il, Oh Mi Hwa, Paik Haemin, Hwang Geon-Tae, No Kwangsoo, Nam Yoon Sung, Lee Keon Jae, Virus-directed design of a flexible $BaTiO_3$ nanogenerator, ACS Nano 7 (12) (2013) 11016–11025.
[17] G.T.P. Hwang, H. Lee, J.H. Oh, S. Park, K.I. Byun, M. Park, H. Ahn, G. Jeong, C. K. No, K. Kwon, H. Lee, S.G. Joung, B. Lee, K. J, Self-powered cardiac pacemaker enabled by flexible single crystalline PMN-PT piezoelectric energy harvester, Adv. Mater. 26 (28) (2014) 4880–4887.
[18] G.-T. Hwang, Kim Youngsoo, Lee Jeong-Ho, Oh SeKwon, Jeong Chang Kyu, Park Dae Yong, Ryu Jungho, Kwon HyukSang, Lee Sang-Goo, Joung Boyoung, Kim Daesoo, Lee Keon Jae, , Self-powered deep brain stimulation via a flexible PIMNT energy harvester, Energy Environ. Sci. 8 (9) (2015) 2677–2684.
[19] C.C. Hu, L. Wang, Z. Zheng, Y. Bai, S.Y. Qin, A transparent antipeep piezoelectric nanogenerator to harvest tapping energy on screen, Small 12 (10) (2016) 1315–1321.
[20] M.Z. Xie, Y. Krasny, M.J. Bowen, C. Khanbareh, H. Gathercole, N, Flexible and active self-powered pressure, shear sensors based on freeze casting ceramic-polymer composites, Energy Environ. Sci. 11 (10) (2018) 2919–2927.
[21] M. Yan, Junwen Zhong, Liu Shengwen, Xiao Zhida, Yuan Xi, Zhai Di, Zhou Kechao, Li Zhaoyang, Zhang Dou, Bowen Chris, Zhang Yan, Flexible pillar-base structured piezocomposite with aligned porosity for piezoelectric energy harvesting, Nano Energy 88 (2021), 106278.

[22] R.Q. Yang, Y. Dai, L. Wang, Z. L, Power generation with laterally packaged piezoelectric fine wires, Nat. Nanotechnol. 4 (1) (2009) 34–39.
[23] X. Yuan, Xiangyu Gao, Jikun Yang, Xinyi Shen, Zhanmiao Li, Sujian You, Zehuan Wang, Shuxiang Dong, The large piezoelectricity and high power density of a 3D-printed multilayer copolymer in a rugby ball-structured mechanical energy harvester, Energy Environ. Sci. 13 (1) (2020) 152–161.
[24] L.L. Gu, J. Cui, N. Xu, Q. Du, T. Zhang, L. Wang, Z. Long, C. Qin, Y, Enhancing the current density of a piezoelectric nanogenerator using a three-dimensional intercalation electrode, Nat. Commun. 11 (1) (2020) 1030.
[25] Z.L. Wang, On Maxwell's displacement current for energy and sensors: the origin of nanogenerators, Mater. Today 20 (2) (2017) 74–82.
[26] Q. Xu, J. Wen, Y. Qin, Development and outlook of high output piezoelectric nanogenerators, Nano Energy 86 (2021), 106080.
[27] S. Hajra, Y. Oh, M. Sahu, K. Lee, H.-G. Kim, B.K. Panigrahi, K. Mistewicz, H.J. Kim, Piezoelectric nanogenerator based on flexible PDMS–$BiMgFeCeO_6$ composites for sound detection and biomechanical energy harvesting, Sustain. Energy Fuels 5 (23) (2021) 6049–6058.
[28] S. Panda, S. Hajra, H. Jeong, B.K. Panigrahi, P. Pakawanit, D. Dubal, S. Hong, H. J. Kim, Biocompatible $CaTiO_3$-PVDF composite-based piezoelectric nanogenerator for exercise evaluation and energy harvesting, Nano Energy 102 (2022), 107682.
[29] J. Yu, S. Xian, Z. Zhang, X. Hou, J. He, J. Mu, X. Qiao, L. Zhang, X. Chou, Synergistic piezoelectricity enhanced $BaTiO_3$/polyacrylonitrile elastomer-based highly sensitive pressure sensor for intelligent sensing and posture recognition applications, Nano Res. (2022) 1–13.
[30] J. Khaliq, Daniella Deutz, Frescas Bayle, Alfonso Jesus, Vollenberg Caraveo, Hoeks Peter, van der Zwaag Theo, Groen, Pim Sybrand, Effect of the piezoelectric ceramic filler dielectric constant on the piezoelectric properties of PZT-epoxy composites, Ceram. Int. 43 (2) (2017) 2774–2779.
[31] F. Qi, N. Chen, Q. Wang, Preparation of $PA_{11}/BaTiO_3$ nanocomposite powders with improved processability, dielectric and piezoelectric properties for use in selective laser sintering, Mater. Des. 131 (2017) 135–143.
[32] M. Taya, A.A. Almajid, M. Dunn, H. Takahashi, Design of bimorph piezo-composite actuators with functionally graded microstructure, Sens. Actuators A Phys. 107 (3) (2003) 248–260.
[33] I. Jung, Youn-Hwan Shin, Sangtae Kim, Ji-young Choi, Chong-Yun Kang, Flexible piezoelectric polymer-based energy harvesting system for roadway applications, Appl. Energy 197 (2017) 222–229.
[34] X. Yu, Yudong Hou, Zan Yang, Xin Gao, Mupeng Zheng, Mankang Zhu, Boosting output current density of piezoceramic energy harvesters using three-dimensional embedded electrodes, Nano Energy 101 (2022), 107598.
[35] A. Dogan, K. Uchino, R.E. Newnham, Composite piezoelectric transducer with truncated conical endcaps "cymbal", IEEE Trans. Ultrason. Ferroelectr. Freq. Control 44 (3) (1997) 597–605.
[36] H.W. Kim, Amit Batra, Shashank Priya, Kenji Uchino, Douglas Markley, Robert Newnham, E. Hofmann, F. Heath, Energy harvesting using a piezoelectric "cymbal" transducer in dynamic environment, Jpn. J. Appl. Phys. 43 (9R) (2004) 6178.
[37] Y. Zhang, Chang Kyu Jeong, Jianjun Wang, Huajun Sun, Fei Li, Guangzu Zhang, Long-Qing Chen, Shujun Zhang, Wen Chen, Qing Wang, Flexible energy harvesting polymer composites based on biofibril-templated 3-dimensional interconnected piezoceramics, Nano Energy 50 (2018) 35–42.
[38] S.-Y. Fu, Xi-Qiao Feng, Bernd Lauke, Yiu-Wing Mai, Effects of particle size, particle/matrix interface adhesion and particle loading on mechanical properties of particulate–polymer composites, Compos. Part B Eng. 39 (6) (2008) 933–961.
[39] H. Gu, Chao Ma, Junwei Gu, Jiang Guo, Xingru Yan, Jiangnan Huang, Qiuyu Zhang, Zhanhu Guo, An overview of multifunctional epoxy nanocomposites. J. Mater. Chem. C 4 (25) (2016) 5890–5906.
[40] J.N. Coleman, U. Khan, Y.K. Gun'ko, Mechanical reinforcement of polymers using carbon nanotubes, Adv. Mater. 18 (6) (2006) 689–706.
[41] F.-L. Jin, X. Li, S.-J. Park, Synthesis and application of epoxy resins: a review, J. Ind. Eng. Chem. 29 (2015) 1–11.
[42] H. Fu, Z. Long, M. Lai, J. Cao, R. Zhou, J. Gong, Y. Chen, Quantum dot hybridization of piezoelectric polymer films for non-transfer integration of flexible biomechanical energy harvesters, ACS Appl. Mater. Interfaces 14 (26) (2022) 29934–29944.
[43] S. Shi, Z. Pan, Y. Cheng, Y. Zhai, Y. Zhang, X. Ding, J. Liu, J. Zhai, J. Xu, Three-dimensional polypyrrole induced high-performance flexible piezoelectric nanogenerators for mechanical energy harvesting, Compos. Sci. Technol. 219 (2022), 109260.
[44] J. Fu, Y. Hou, M. Zheng, M. Zhu, Flexible piezoelectric energy harvester with extremely high power generation capability by sandwich structure design strategy, ACS Appl. Mater. Interfaces 12 (8) (2020) 9766–9774.
[45] Z. Hanani, I. Izanzar, M.'b Amjoud, D. Mezzane, M. Lahcini, H. Uršič, U. Prah, I. Saadoune, M.E. Marssi, I.A. Luk'yanchuk, Z. Kutnjak, M. Gouné, Lead-free nanocomposite piezoelectric nanogenerator film for biomechanical energy harvesting, Nano Energy 81 (2021), 105661.
[46] Z. Zhou, Q. Zhang, Z. Zhang, H. Kuang, X. Du, H. Yang, Lead-free, high-current output piezoelectric nanogenerators using three-dimensional interdigitated electrodes, Chem. Eng. J. 442 (2022), 136241.

Binbin Ma received his B.S. degree in Metal Material Engineering from China Three Gorges University, Now he is a doctoral candidate in the School of Materials and Energy, Lanzhou University. His research mainly focuses on piezoelectric nanogenerators.

Li Cheng received his B.S. (2011) in Physics and Ph.D. (2016) in Material Physics and Chemistry from Lanzhou University. Now he is an associate professor in School of Materials and Energy of Lanzhou University at Institute of Nanoscience and Nanotechnology. His research mainly focuses on nanogenerators and self-powered nanodevices.

Suo Bai received his B.S. (2008) in Material Physics and Ph.D. (2014) in Material Physics and Chemistry from Lanzhou University, China. Now he is an associate professor in School of Materials and Energy of Lanzhou University at Institute of Nanoscience and Nanotechnology. His research focuses on fabrication of nanodevices and self-powered nanodevices.

Xiaofeng Jia received his B.S. degree in Materials Chemistry from Tianjin University of Technology (2013) and Ph.D. degree in Materials Physics and Chemistry supervised by Prof. Yong Qin from Lanzhou University (2021). He is currently a process engineer at Guangzhou CanSemi Technology Inc., and his work focuses on the thin film deposition in chip fabrication.

Jun Ma received his B.S. from the School of Materials Science and Engineering, Xi 'an University of Science and Technology in 2018. He is now a Ph.D. candidate at the School of Materials and Energy, Lanzhou university. His research interests focus on liquid-solid contact tribovoltaic effect and triboelectric nanogenerator for blue energy.

Jiling Zhao received his M.Eng. from the School of Metallurgy and Energy Engineering, Kunming University of Science and Technology in 2020. He is now a doctoral candidate at the School of Materials and Energy, Lanzhou University. His research focuses on preparation of nanomaterials and their applications in the selective separation and recovery of pollutants and noble metals.

Longfei Wang received his B.S. (2012) in Materials Science and Engineering from China University of Geosciences (Beijing) and Ph.D. (2017) in Nanoscience and Technology from Beijing Institute of Nanoenergy and Nanosystems, Chinese Academy of Sciences. He is now a postdoctoral fellow in Professor Zhong Lin Wang's group at Georgia Institute of Technology. His current research focuses on interfacial polarization (opto)electronics of semiconductors such as piezotronics and piezo-phototronics, and flexoelectronics.

Yong Qin received his B.S. (1999) in Material Physics and Ph. D. (2004) in Material Physics and Chemistry from Lanzhou University. From 2007–2009, he worked as a visiting scholar and Postdoc in Professor Zhong Lin Wang's group at Georgia Institute of Technology. Currently, he is a professor at the Institute of Nanoscience and Nanotechnology, Lanzhou University, where he holds a Cheung Kong Chair Professorship. His research interests include nanoenergy technology, functional nanodevice and self-powered nanosystem. Details can be found at: http:// www.yqin.lzu.edu.cn.